

This article was downloaded by: [UNAM Ciudad Universitaria]

On: 08 April 2015, At: 10:00

Publisher: Taylor & Francis

Informa Ltd Registered in England and Wales Registered Number: 1072954 Registered office: Mortimer House, 37-41 Mortimer Street, London W1T 3JH, UK



Tribology Transactions

Publication details, including instructions for authors and subscription information:

<http://www.tandfonline.com/loi/utrb20>

Preliminary Tribological Study and Tool Life of Four Commercial Drills

Marco Figueroa^{ab}, Ernesto García^{ab}, Stephen Muhl^b & Sandra Rodil^b

^a Sección de Estudios de Posgrado e Investigación Escuela Superior de Ingeniería Mecánica y Eléctrica Instituto Politécnico Nacional, Gustavo A. Madero 07738, México

^b Instituto de Investigaciones en Materiales Universidad Nacional Autónoma de México, Coyoacán 04510, México

Accepted author version posted online: 18 Feb 2014. Published online: 15 Apr 2014.



CrossMark

[Click for updates](#)

To cite this article: Marco Figueroa, Ernesto García, Stephen Muhl & Sandra Rodil (2014) Preliminary Tribological Study and Tool Life of Four Commercial Drills, Tribology Transactions, 57:4, 581-588, DOI: [10.1080/10402004.2014.887166](https://doi.org/10.1080/10402004.2014.887166)

To link to this article: <http://dx.doi.org/10.1080/10402004.2014.887166>

PLEASE SCROLL DOWN FOR ARTICLE

Taylor & Francis makes every effort to ensure the accuracy of all the information (the "Content") contained in the publications on our platform. However, Taylor & Francis, our agents, and our licensors make no representations or warranties whatsoever as to the accuracy, completeness, or suitability for any purpose of the Content. Any opinions and views expressed in this publication are the opinions and views of the authors, and are not the views of or endorsed by Taylor & Francis. The accuracy of the Content should not be relied upon and should be independently verified with primary sources of information. Taylor and Francis shall not be liable for any losses, actions, claims, proceedings, demands, costs, expenses, damages, and other liabilities whatsoever or howsoever caused arising directly or indirectly in connection with, in relation to or arising out of the use of the Content.

This article may be used for research, teaching, and private study purposes. Any substantial or systematic reproduction, redistribution, reselling, loan, sub-licensing, systematic supply, or distribution in any form to anyone is expressly forbidden. Terms & Conditions of access and use can be found at <http://www.tandfonline.com/page/terms-and-conditions>

Preliminary Tribological Study and Tool Life of Four Commercial Drills

MARCO FIGUEROA,^{1,2} ERNESTO GARCÍA,^{1,2} STEPHEN MUHL,² and SANDRA RODIL²

¹Sección de Estudios de Posgrado e Investigación
Escuela Superior de Ingeniería Mecánica y Eléctrica
Instituto Politécnico Nacional, Gustavo A. Madero 07738, México

²Instituto de Investigaciones en Materiales
Universidad Nacional Autónoma de México
Coyoacan 04510, México

The mechanical and tribological properties of drill bits have a strong influence on the characteristics and performance of such tools. Today there are many different types and makes of drills available and their various characteristics influence their efficiency and, of course, their cost. In this preliminary project, four commercial drills were studied; multiple examples of two of the drills were tested. These were selected because of their price and characteristics from those available in the Mexican national market. The tools were submitted to a variety of characterization tests in order to determine their mechanical and tribological behaviors. The tests included hardness by indentation (both micro- and nanotesting), microabrasion by ball cratering, and scratch testing to determine the coating adherence and surface scratch resistance by novel scratch testing procedure. Additionally, the drills were analyzed by energy-dispersive X-ray spectroscopy (EDX), Rutherford backscattering (RBS), and scanning electron microscopy to determine the surface characteristics and composition. The tracks resulting from the tribological tests were studied by profilometry and optical microscopy. The performance of the drill bits was then tested using a vertical drilling machine under controlled conditions of fixed cutting speed, constant load, and drilling depth. The quality of the drilled holes was determined by measuring the difference between the upper and lower diameters of the holes. We found that the wear rate, measured by ball cratering, and the bulk hardness rather than the surface hardness of the drill bits correlated best with the drill performance and lifetime.

KEY WORDS

Boring; Ball Cratering; Scratch Testing; Hardness Tests; Drill Lifetime

INTRODUCTION

In the manufacturing industry drilling is one of the principal operations and studies have shown that more of 25% of the manufacturing time is spent on drilling processes (Wang and Zhang (1); Faraz, et al. (2)). Drilling has been used since Ancient Egyptian times and in the modern era many studies have been performed to improve the efficiency of this operation. Furthermore, drilling is a complicated operation because it involves a three-dimensional asymmetric cutting tool and the tool life is dependent on a large number of factors related to the design of the tool, the tool material and coatings, the conditions under which the drills are operated and the material to be perforated (Shen, et al. (3)). It is estimated that approximately 250 million drill bits are used annually in the U.S. industry alone. The wear to the drill bit during its use is a progressive and comparatively slow phenomenon, whereas tool failure and breakage of the cutting edge are usually catastrophic and happen with little warning. Even though a drill begins to wear as soon as it is placed into operation, the wear occurs at an accelerated rate once it becomes dull (Huseyin, et al. (4)). Wear initially takes place at the outer margin of the flutes of the drill due to the intimate contact and elevated temperatures at the tool point of contact with the material being machined. However, drill wear differs to some extent from the wear of other cutting tools due to the fact that drills are slightly asymmetric; therefore the bit only wears at one lip until the height of both lips are equal (Pluta and Hryniewicz (5)). The second lip then becomes sharper and becomes the cutting edge. This alternating process occurs almost throughout the drill lifetime. In the end the drill sticks in the workpiece and tool breakage can occur if the process is not stopped (Jantunen (6)).

In recent years, thin layers of hard and wear-resistant coatings, such as titanium nitride (TiN), have been deposited on the surface of HSS drills to increase the drill life and cutting efficiency (Wang and Zhang (1)). Since the early 1980s such hard coatings deposited by physical vapor deposition, using ion plating with low- or high-voltage electron beam source, cathodic arc evaporation, or, more recently, magnetron sputtering techniques, have become increasingly commercially available. The intrinsic wear-resistant properties, inertness, and aesthetically pleasing appearance of

titanium nitride (TiN), the first widely used industrial coating, have made it attractive for a range of applications, including cutting tools of various types (Minevich, et al. (7)). In the last few years, nanostructured coatings have been developed and are reported to improve the properties of drills even more (Smith, et al. (8)).

On the other hand, the forces involved in the cutting process are often monitored in order to determine the development of cutting tool wear. In general, it is known that the cutting forces increase as tool wear increases due to the increase in friction between the tool and the workpiece (Cantero, et al. (9); Mori, et al. (10)). In drilling it is possible to monitor the torque, drift forces, feed force, vibrational signal, as well as electrical power used by the drilling machine (Rawat and Attia (11)).

In this study we have investigated the relationship between the measureable physical and tribological characteristics and the performance of four commercially available drill bits. We have characterized the performance by measuring the energy consumption during use, tool life, and quality of the holes cut in a 20-mm-thick carbon steel plate. The drilling conditions chosen for this study were similar to those commonly used for conventional drill press or hand drilling rather than that for a modern computer numerical control (CNC) machine tool. We also present a novel use of scratch testing to provide a measure of the wear resistance of the drill bits. The principal aim of this study is to identify which physical/tribological properties, or combination of properties, is most useful to predict the performance of a drill bit.

EXPERIMENTAL DETAILS

In the Mexican market, various different types of drills are available but the variety is considerably smaller than in the United States or Europe. For this project, four 12.7-mm-diameter drills of the same geometry were selected; in particular, all of the drills had the same shank spiral, tip point angle, and cutting edge lip angles; additionally, we ensured that we included the most expensive and cheapest drills that are readily available. Unfortunately, at the time of this study multiple drills of only two of the types of drills, referred to as B1 and B3, were available. The error bars in the various graphs of the results indicate the uncertainty determined from measurements on the multiple drills. The chemical composition of the drills and the surface coatings was determined by energy-dispersive X-ray spectroscopy (EDX) and Rutherford backscattering (RBS), the latter using a 1.5 MeV deuterium beam.

The hardness of the shank, close to the tip, was measured by microindentation using an LM700, LECO Micro Hardness Tester; five tests per drill bit were performed using loads from 0.0981 to 9.81 N and a 30-s dwell time. The measurements were made approximately 5 mm from the tip before the drill was used. Additionally, six nanoindentation tests per drill bit were carried out using a CSM nanoindenter with a load of 10 mN. Because the indentation tests were carried out on the curved surface of the 12.7-mm-diameter drills some distortion of the pyramidal Vicker's indentation marks was inevitable. Using a basic geometrical calculation of the dimensions of the diagonal of the indentation marks for hardness of 1,000 and 580 HV and

using the relationship,

$$HV = 1.85 \times F \text{ (kgF)} / d^2 \text{ (mm)}.$$

Assuming that the indentation depth was one seventh of the diagonal, we obtained that for a load of 9.8 N the expected diagonal on a flat surface, for a hardness of 1,000 HV, would be $\sim 43 \mu\text{m}$ and on the curved surface of the drill the projected length (the length obtained from a normal optical microscope measurement) of the diagonal would be $\sim 42.8 \mu\text{m}$ and for the 580 HV hardness the flat diagonal would be $\sim 56.5 \mu\text{m}$ and the projected length on the curved surface was calculated to be $56.1 \mu\text{m}$. We consider that such errors were acceptable and considering that at least 10 measurements were taken on each drill shank and that the average of the two diagonals was used to calculate the hardness (one of the diagonals being aligned along the drill axis), we believe that the values of hardness are representative of the drills. The microhardness results for the lowest loads are a combination of the hardness of the bulk and surface and the hardness value of the bulk, or interior of the drill, was taken to be the almost constant value obtained for the highest indentation loads. For the nanoindentation measurements, care was taken to ensure that the indentation was performed at the highest point of the curved surface so that the penetration was as uniform as possible.

Ball cratering is a well-established technique for generation of microabrasion by means of the rotation of a steel ball continuously fed by an abrasive slurry. In general, a suspension of hard particles in water was used as the slurry to generate the wear crater (Gee, et al. (12)). The wear rate is normally measured by calculating the volume of crater,

$$V = \pi b^4 / 64R,$$

where b is the crater diameter and R is the ball radius ($b \ll R$). However, the above equation could not be applied to our samples because of the curvature of the drill surface, which resulted in elliptical wear marks. Therefore, the following equation was used:

$$\text{Volume of crater: } V = \frac{2}{3} \pi a b d,$$

where a and b are the length of the two axes of the ellipse and d is crater depth (Ramalho (13); Lou, et al. (14)).

$$d = R - \left(R^2 - \left(\frac{a}{2} \right)^2 \right)^{1/2}.$$

In the experiments, three tests were performed for each load of 1.03, 2.02, 3.05, 4.08, and 5.11 N on each of the drill bits. The wear rate of the drill bits was obtained by calculating the average volume from the dimensions, measured using a DekTak 150 profilometer, of the craters generated by 1,000 revolutions of a 2.54-cm-diameter hard steel ball with a continuous supply of a slurry made from a 2 wt% concentration of 0.1- μm diamond powder colloidal suspension in deionised water. The total test distance was 80 m at rotation velocity of 100 rpm.

Scratch testing was carried out using a Rockwell C diamond tip in a Tribotechnic Millenium 100 machine up to a maximum load of 80 N. All scratches were performed parallel to the axis of the drill bit starting approximately 5 mm from the tip of the drill

bit. The profiles of the surface scratches were measured using profilometry. Scratch testing is commonly used to assess the adhesion of coatings to a substrate (Duan, et al. (15)). However, it can also be used to estimate the scratch resistance of a material (Sander, et al. (16); Li and Beres (17); Rawers, et al. (18)) and in Bautista, et al. (19) the scratch and wear resistance of organic coatings is compared. Our test procedure consisted of normal scratch measurements, 6 mm long, translation speed of 24 mm/min, using an increasing load from 0 to 80 N. The cross-sectional profiles of the scratches were then measured at 20 different positions along the scratch using the profilometer. The depth of the scratch was plotted against the load (distance) for each drill. We propose a novel way of describing the scratch wear resistance of a material by using the value of the gradient of the linear plastic deformation section of the scratch depth vs. load plots. If a material has a high resistance to scratching (plastic deformation), then the depth of the scratch should only increase slowly as the scratch load is increased, with this resulting in a small value of the scratch load gradient.

Finally, the lifetime and drilling efficiency of the four drill bits was determined. Care was taken to ensure that the same drilling conditions were used for each of the drills. The drills were used to perforate holes in 20-mm-thick plate of carbon steel (hardness 161 HV) and 14.1-mm-thick plate of stainless steel (hardness 277 HV). A vertical drill press (Arboga Maskiner, U 2508, three phases, 220 V, 3,420/1,700 rpm) was used with the following drilling test parameters: for the carbon steel, the spindle velocity was 530 rpm with a load of 630 N; for the stainless steel, the spindle velocity was 250 rpm and the load was 1,680 N. No lubricant was used for either material. For modern CNC drilling the spindle velocity and penetration velocity are controlled but the applied force is a variable. However, for low-volume jobs, manual or semi-automated drilling is often used and for those processes the applied force is frequently controlled and constant.

Initially, various exploratory test holes, using a 3/8" drill, were made in the two plates to check whether there were any obvious inhomogeneities in the steel. Then up to 60 holes were drilled in the carbon steel using the four 12.7-mm-diameter test drills. For those drills that were still useable, additional perforations were made in the stainless steel plate. The following procedure was used to reduce the effect of the impact damage when the drill was initially placed in contact with the workpiece: firstly, the drill was brought into contact with the steel, the load was applied, and then the drilling machine was turned on and the drill was allowed to perforate the metal plate at whatever rate it was capable of achieving. To avoid variation in the drilling procedure due to the drill temperature, the drill bit was allowed to cool to close to room temperature before the next hole was drilled. During the drilling operation, the electrical current used by the drilling machine was recorded and the time to complete each hole was measured. After drilling, both the characteristics of the drill bits and the holes in the carbon steel were measured. In particular, the dimensions of upper and lower extremes of each hole were measured in order to try to assess the uniformity and quality of the drilled holes. Optical images were taken of the drill bits after drilling. For the EDX/scanning electron microscopy work, a 5-mm-thick cross-sectional piece was cut from each drill bit and

the center area of each piece was used to determine the bulk composition of the steel by EDX.

RESULTS AND DISCUSSION

Chemical Composition

The elemental analysis of the drill bits indicated that all four drill bits had different surface and bulk chemical compositions. Table 1 shows the details of the thickness and composition of the surface layers determined by RBS, together with the bulk composition of the steel used for the drill shaft measured by EDX. It should be noted that the EDX system used could not detect elements lighter than nitrogen and the RBS measurements indicated that the drill shaft material contained approximately 5% carbon. The bulk composition of the drills is fairly typically of high-speed steel. Drills B1 and B2 had 1.5- to 2.0- μm -thick surface coatings of TiN and CrN, respectively, as well as an interface layer of graded composition of thickness of 1.5–3.7 μm . Drills B3 and B4 had a highly oxidized surface layer, 1.0–1.5 μm , and a graded oxide interface layer, 2.1–2.5 μm , probably produced by tempering; unfortunately, the drill fabrication companies would not provide any information concerning the heat treatments used on their drills.

Hardness

The hardness results are shown in Fig. 1. For drill bits B1 and B2, nanoindentation measurements were performed using a load of 10 mN in order to determine the hardness of the coating; see Fig. 1. The apparatus also calculates the Young's modulus and

TABLE 1—CHEMICAL COMPOSITION OF THE FOUR DRILLS. THE RBS DATA GIVE THE COMPOSITION AND THICKNESS OF THE SURFACE LAYERS AND THE EDX DATA ARE FOR THE BULK DRILL BIT

	B1	B2	B3	B4
Surface (RBS)				
Layer 1 thickness	1.5 μm	2.0 μm	1.0 μm	1.5 μm
Elements (at%)				
Ti	50.0	—	—	—
Cr	—	34.0	—	—
N	50.0	66.0	—	—
O	—	—	15.0	27.0
Fe	—	—	85.0	73.0
Layer 2 thickness	1.5 μm	3.7 μm	2.5 μm	2.1 μm
Elements (at%)				
Ti	30.0	30.0	3.5	—
Fe	10.0	5.0	32.0	20.15
C	18.5	10.0	18.0	40.0
N	21.5	43.0	—	—
O	20.0	12.0	46.0	39.7
W	—	—	0.5	0.15
Bulk (EDS)				
Elements (at%)				
Fe	89.09	88.4	94.43	95.26
V	3.39	3.32	3.39	3.48
S	2.17	—	—	—
W	5.36	1.59	2.18	1.26
Ti	—	6.1	—	—

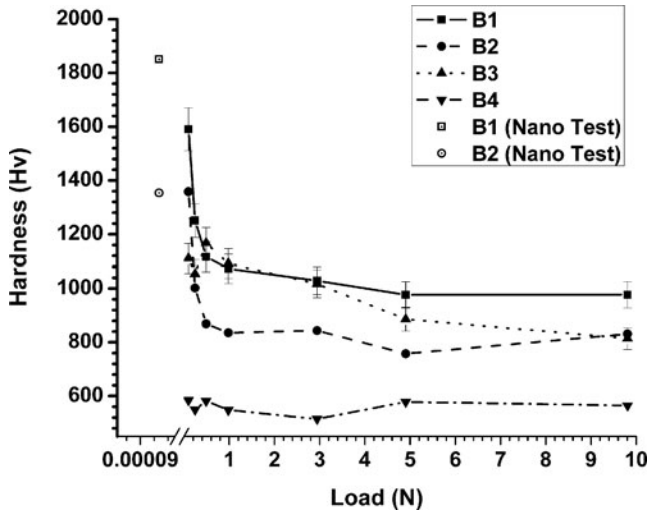


Fig. 1—Nano- and microhardness of the four drill bits as a function of the applied load.

gave values of 286 and 255 GPa for B1 and B2, respectively. The maximum nanoindentation depth was 180 nm for B1 and 205 nm for B2 and these are both approximately 1/10 of the nitride coating thickness, which means that the hardness values are a good representation of the hardness of the surface coating. It can be seen that the microhardness tests gave similar bulk hardness of $\sim 1,000$ HV of drills B1 and B3 but the low-load or near-surface hardness of B1 at $>1,800$ HV was much larger. The other coated drill B2 also had a high near-surface hardness of $\sim 1,400$ HV but the bulk hardness was ~ 800 HV. The low-cost drill B4 was the softest at ~ 580 HV and the hardness did not increase for low-indentation loads. The three drills B1, B2, and B3 all showed increased hardness values for the lowest microhardness loads; for B1 and B2 this was due to the hard coating and for B3 this was probably a result of thermal annealing.

Ball Cratering

The results of the ball cratering tests are presented in Fig. 2. The wear rates of drills B1, B2, and B3 are quite similar and were less than 1.2×10^{-4} mm³/m; additionally, the wear rates did not strongly increase as the load increased. The calculated standard deviation of this data is approximately 2.0×10^{-6} mm³/m and, therefore, the wear resistance of B1 is the best, followed by B3 and then B2. Drill B4 had an order of magnitude worse wear resistance and the wear increased almost linearly with increasing load. It should be mentioned that under the test conditions used the final crater depth for drills B1, B2, and B3 was approximately 3 μ m, which was less than, or similar to, the thickness of the hard coatings on the drills B1 and B2 and, based on the indentation data, was less than the surface-hardened layer produced by thermal annealing of drill B3.

Scratch Test

The results for the four drill bits are given in Figs. 3a and 3b. Figure 3a shows the depth of the scratch, measured by profilometry, for the load range of 0 to 80 N for the four drill bits. A linear fit to the data for each bit was calculated and the value of

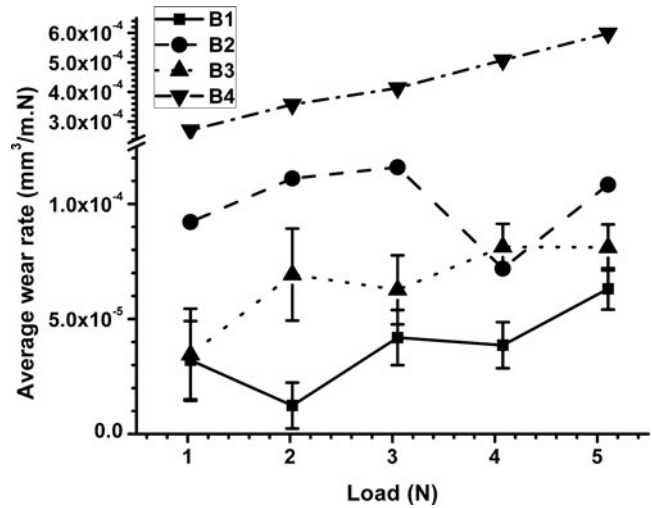


Fig. 2—Average wear rate from the ball cratering measurements on the four drill bits against the applied load.

this slope is plotted in Fig. 3b; data were included from the three smaller load ranges; 0–60 and 0–40 N. For drill B4, which had the lowest scratch resistance, there is considerable spread in the depth data; however, the linear fit still gives an R^2 value of 0.95 (see Fig. 3a). The linear fit to the other data sets is considerably better. The results given in Fig. 3b show that drill bits B1, B2, and B3 have similar high values of scratch resistance. For the highest scratch test load the scratch resistance of drill B1 is somewhat better than that of B2 and B3. The drill B4 has more than an order of magnitude worse scratch resistance.

Drill Performance

Figure 4 shows the results of the drilling tests for the four drill bits under the conditions described earlier. Both B1 and B3 drills were capable of producing the 60 holes in carbon steel plate; however, only three holes could be made by drill B4 and 38 by drill B2. Eleven additional holes could be made in the stainless steel plate using B1 and four holes were possible with drill B3. The characteristics of failure were almost identical for all of the drills; that is, after the initial slow penetration of the drill point into the steel no further advance was observed—the drill became so worn that it stopped cutting.

Figures 5a–5c show the temporal variation of AC current used by the drilling machine to produce the first, 30th, and 60th holes in the carbon steel. Various details of the cutting ability of the drills can be obtained from these plots. Firstly, the time to cut the first hole was approximately 36 s for B1, 53 s for B3, 72 s for B2, and 168 s for B4. The value of the AC current is an indication of the cutting efficiency of the drill bits and it can be seen that the efficiency of B1 and B3 were similar but the drill bit B2 was less efficient and therefore more electrical current was needed. Drill B4 initially required a low AC current but took much longer to perforate the steel plate and the current strongly increased at the end of the perforation. The same pattern was seen for all three holes that were possible with the B4 drill bit; the current was initially 1.85–2.1 A, and drilling times of 170, 300, and 260 s were observed for the first, second, and third holes.

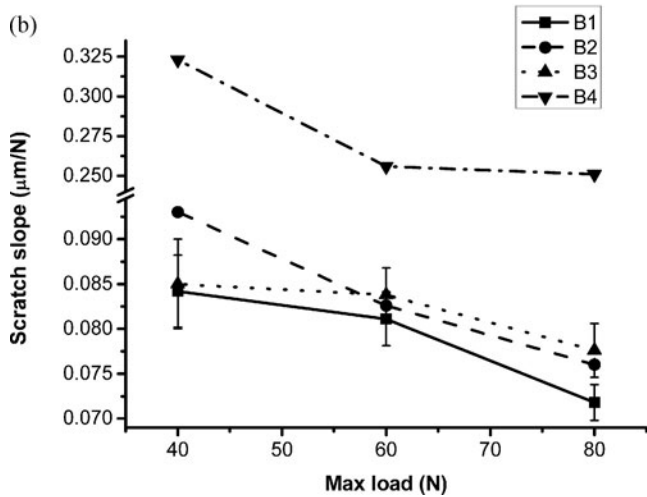
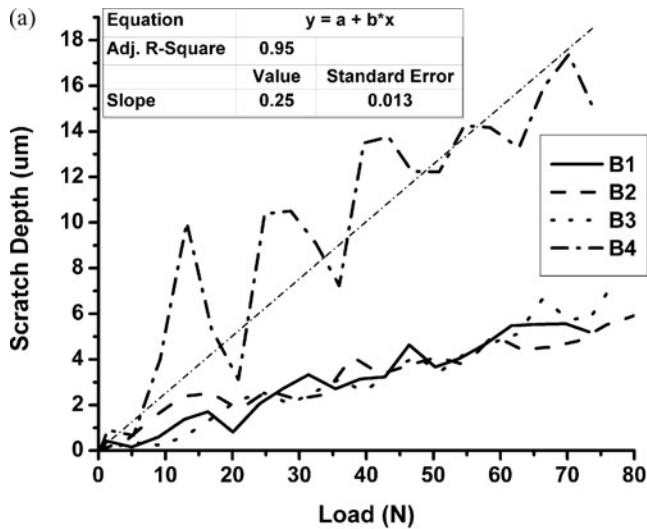


Fig. 3—(a) Variation in the scratch depth versus the applied load for the four drills. The dotted line is a straight line fit to the data for drill bit B4 and the box shows the associated information. (b) Slope of the scratch depth vs. load plotted against the maximum load applied in the scratch test experiment for the four drill bits.

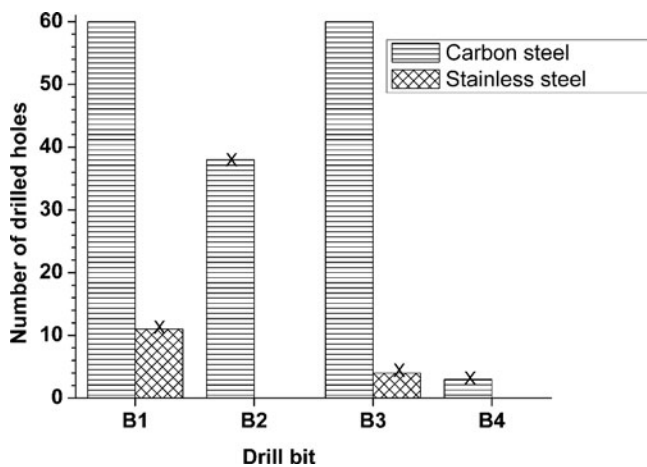


Fig. 4—Number perforations performed in the carbon steel and stainless steel plates by each drill bit. The “X” indicates when the drill bit failed.

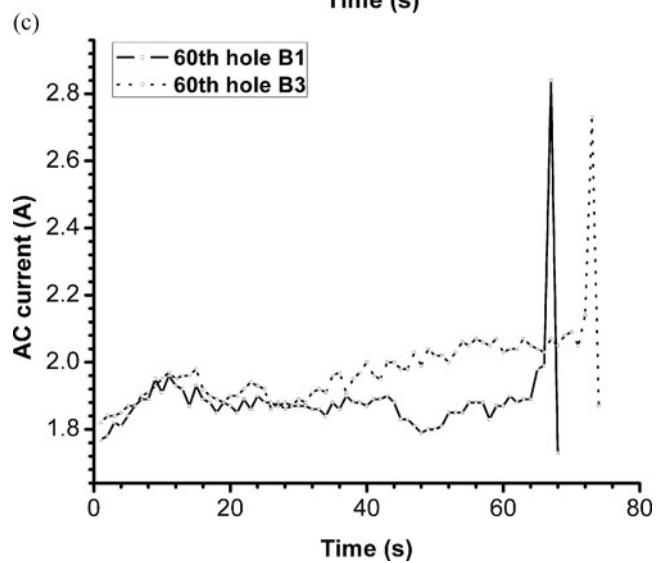
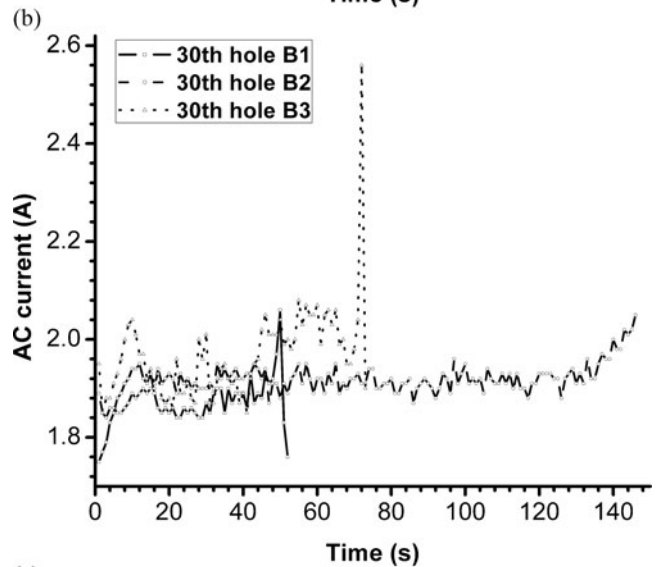
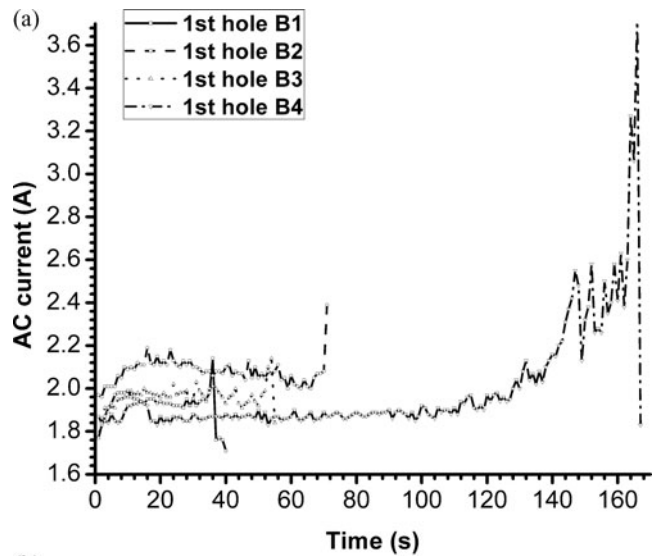


Fig. 5—Temporal variation of the AC electrical current supplied to the drilling machine during the boring of a hole by each drill bit: (a) the first hole, (b) the 30th hole, and (c) the 60th hole.

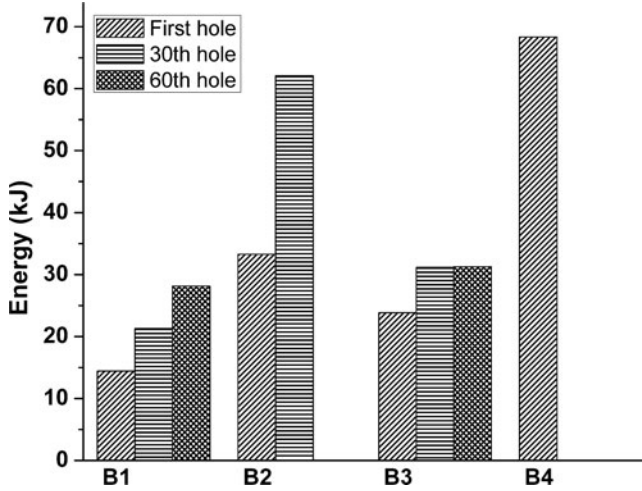


Fig. 6—Electrical energy (the product of the AC current, AC voltage, and time to make the hole) used to make the first, 30th, and 60th hole for each drill bit.

It can be seen that the ordering of the times to perforate the steel plate for the first, 30th, and 60th holes was always B1 the fastest, followed by B3 and then B2, with the currents being fairly similar for the three drills, and this did not strongly change as a function of the number of perforations. From the data we calculated the energy required to perforate the plate and this is plotted in Fig. 6 for the first, 30th, and 60th holes. The drilling ability of the four drill bits can be seen and, as expected, more energy was required as more holes were drilled. Bits B1 and B3 showed similar performance but, somewhat surprisingly, the uncoated drill bit B3 showed the same energy requirement for holes 30 as 60, which indicated that the cutting edges of the drill did not appear to greatly suffer from progressive wear.

Figure 7 shows the time required to make each perforation. As seen in Fig. 5a, drill bit B4 took much longer to drill each of the three holes that were possible. The drilling time per hole for

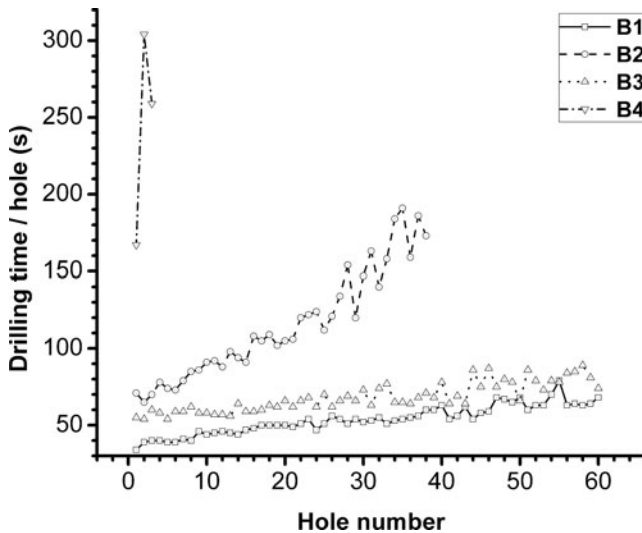


Fig. 7—Time that each drill took to make each perforation.

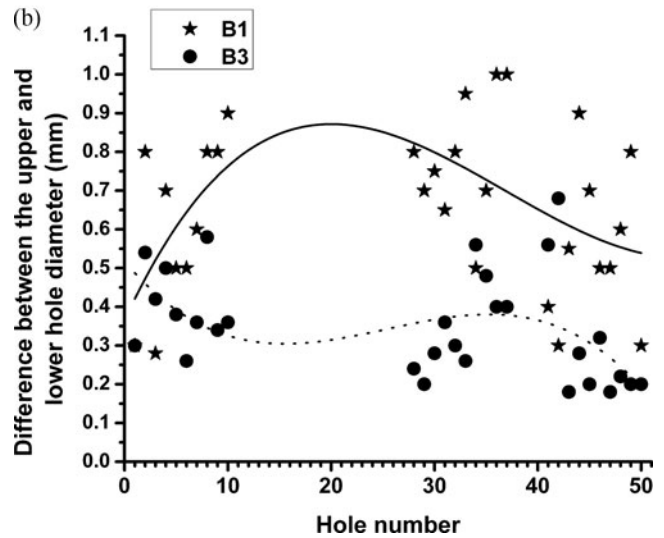
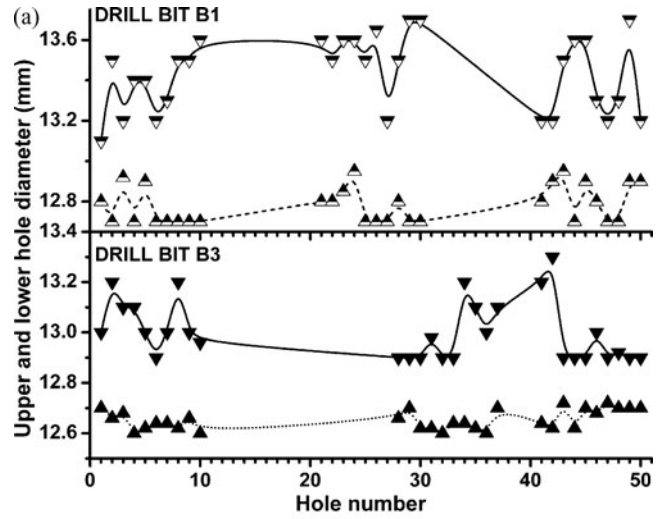


Fig. 8—Representation of the quality of the drilling process: (a) upper and lower diameter of each perforation for drill bits B1 and B3; the lines are spline fits to the data as aid to the eye; and (b) difference between the upper and lower diameters of the perforations; the lines are a polynomial fit to the data.

the 60 perforations was lowest for drill bit B1, followed by B3, and for both of these bits the drilling times increased by about 66 and 55%, respectively. The drilling time for B2 was somewhat longer but increased by ~150% for the last (38th) possible hole.

As mentioned earlier, we estimated the quality of the drilling by measuring the upper and lower diameters of a selection of the holes made using the drill bits B1 and B3; see Fig. 8a. In all cases the upper diameter was larger than the lower one, indicating that a certain amount of distortion of the drill bit occurred during the drilling process. Figure 8b is a plot of the difference between the two diameters, Δd , for each of the 50 holes. Although there is a large degree of dispersion in the data it is clear that the quality (uniformity) of the holes made by drill B3 was better than B1. The data for drill bit B2 were not included because all values of Δd were greater than 0.7 mm.

Figures 9–9d show optical microscope images of the four drill bits after their use. Quite considerable damage can be observed in the four cases but the rounding of the cutting edges and the point or web of the drills B2 and B4 is more pronounced than for bits B1 and B3, and for these bits the damage to the shank is more notable, possibly due to the more extensive use.

Table 2 contains a compilation of the characteristics of the drill bits with the drilling performance of each. The TiN-coated drill, B1, had the best tribological characteristics and showed the best tool lifetime; however, the uncoated drill, B3, also gave a good tool performance. Indeed, in terms of the quality of drilling (change in the drilling time and variance in the diameter of the drilled hole), bit B3 was somewhat better than B1.

It is notable that the bulk and surface hardness, wear rate, and scratch resistance of the drill bits were related to the drill lifetime, drilling efficiency, and perforation time but not to the quality of the drilled hole. However, the scratch resistance was the same for drills B2 and B3 and the surface hardness of B2 was greater than B3, even though B3 had a longer lifetime, better drilling efficiency, and shorter perforation time. Consequently, the bulk hardness and ball cratering wear rate appear to be best related to the drill performance. Finally, apparently none of the

TABLE 2—RELATIVE MECHANICAL AND TRIBOLOGICAL CHARACTERISTICS OF THE FOUR DRILLS AND THE PERFORMANCE OF THE SAME DRILLS

	B1	B2	B3	B4
Drill bit characteristics				
Surface hardness (GPa)	1,850	1,350	1,140	580
Bulk hardness (GPa)	970	760	940	580
Wear rate @ 5N (mm ³ /m × 10 ⁻⁵)	6	11	8.1	60
Average scratch resistance (μ(m/N × 10 ⁻²))	7.8	8.3	8.2	26.0
Drill bit performance				
Max. number of holes, carbon steel	60	38	60	4
Max. number of holes, stainless steel	11	—	4	—
Drilling efficiency {Energy/30th hole (kJ)}	22	62	31	—
Time to drill last hole (s)	69	180	82	260
Percentage change in drilling time (%)	66	150	55	—
Difference between the upper and lower hole diameters	0.57	—	0.23	—

Note. The bold/italic numbers are the best values for each characteristic.

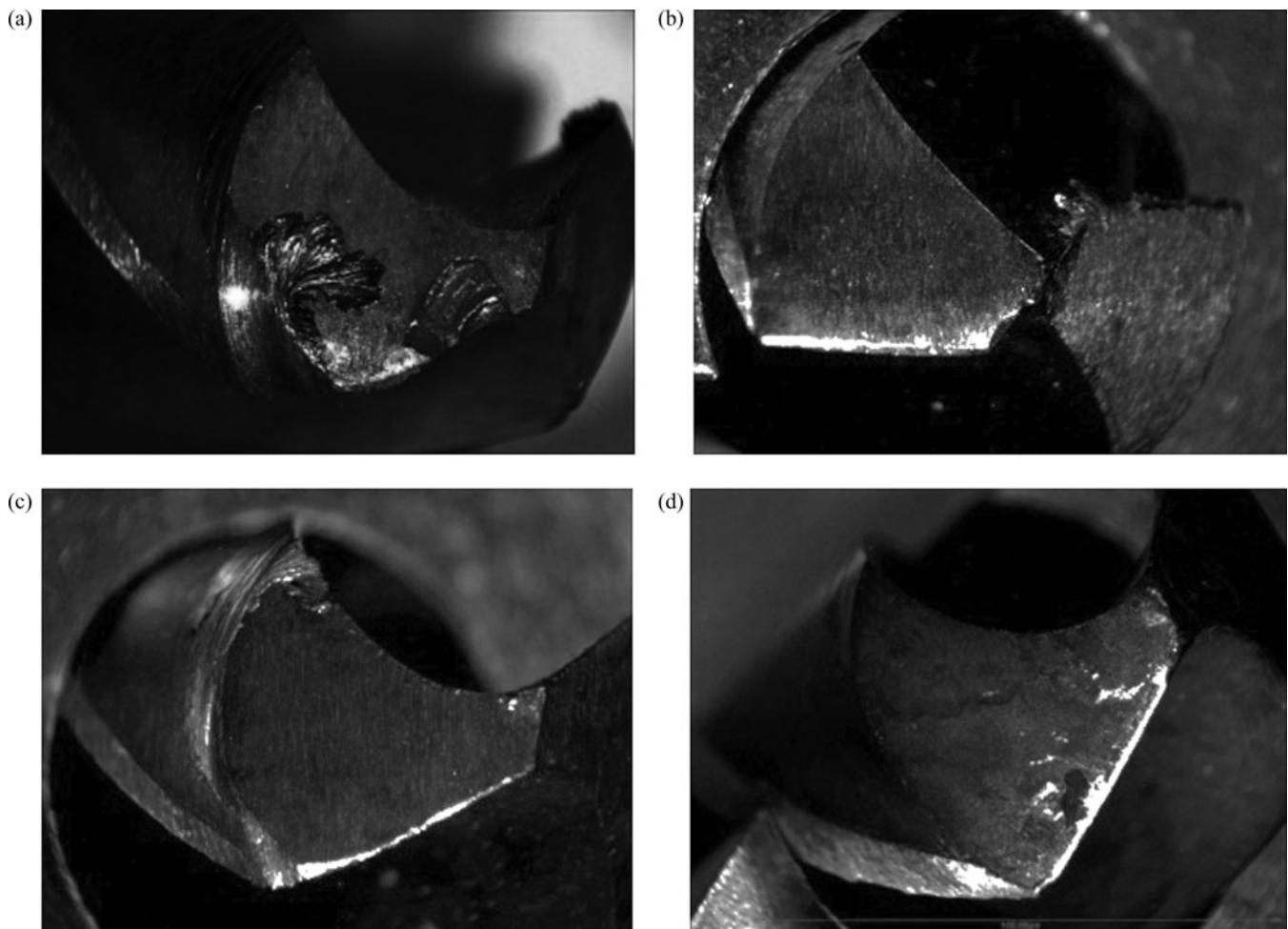


Fig. 9—Photographs of the damage to the points of the drills after use: (a) B1, (b) B2, (c) B3, and (d) B4.

measured characteristics could be used to predict the quality of the drilled hole.

CONCLUSIONS

Four commercially available drill bits were tested under the same drilling conditions to identify the most important drill bit characteristics to aid in the prediction of the performance of the bit and the quality of the drilled holes. It was found that the surface hardness of the bits was not a good indicator but both the bulk hardness and the ball crater wear rate agreed well with the drill bit performance. However, with the characterization techniques used it was not possible to establish a clear relation with the quality of the drilled hole. A notable conclusion was that drills with hard coatings are not necessarily better than good-quality uncoated drills.

FUNDING

The authors acknowledge financial support of the DGAPA-UNAM Project Nos. IN112111 and IN112608.

REFERENCES

- (1) Wang, J. and Zhang, Q. (2008), "A Study of High-Performance Plane Rake Faced Twist Drills. Part I: Geometrical Analysis and Experimental Investigation," *International Journal of Machine Tools & Manufacture*, **48**, pp 1276–1285.
- (2) Faraz, A., Biermann, D., and Weinert, K. (2009), "Cutting Edge Rounding: An Innovative Tool Wear Criterion in Drilling CFRP Composite Laminar," *International Journal of Machine Tools & Manufacture*, **45**, pp 1185–1196.
- (3) Shen, Q., Lau, W. S., and Lee, T. C. (1997), "Study on the Tool Life of Spade Drill with and without a Chip Break," *Journal of Material Processing Technology*, **63**, pp 193–198.
- (4) Huseyin, M., Ertunc, H. M., Loparo, K. A., and Ocak, H. (2001), "Tool Wear Condition Monitoring in Drilling Operations Using Hidden Markov Models (HMMs)," *International Journal of Machine Tools & Manufacture*, **41**, pp 1363–1384.
- (5) Pluta, Z. and Hryniewicz, T. (2012), "Novel Modeling of Tool Edge Wear," *Tribology Transactions*, **55**, pp 230–236.
- (6) Jantunen, E. (2002), "A Summary of Methods Applied to Tool Condition Monitoring in Drilling," *International Journal of Machine Tools & Manufacture*, **42**, pp 997–1010.
- (7) Minevich, A. A., Eizner, B. A., Gick, L. A., and Popok, N. N. (2000), "Case Studies on Tribological Behavior of Coated Cutting Tools," *Tribology Transactions*, **43**, pp 740–748.
- (8) Smith, I. J., Gillibrand, D., Brooks, J. S., Münz, W. D., Harvy, S., and Goodwin, R. (1997), "Dry Cutting Performance of HSS Twist Drills Coated with Improved TiAlN," *Surface and Coating Technol.*, **90**, pp 164–171.
- (9) Cantero, J. L., Tárdio, M. M., Canteli, J. A., Marcos, M., and Miguélez, M. H. (2005), "Dry Drilling of Alloy Ti-6Al-4V," *International Journal of Machine Tools & Manufacture*, **45**, pp 1245–1255.
- (10) Mori, M., Fujishima, M., Inamasu, Y., and Oda, Y. (2011), "A Study on Energy Efficiency Improvement for Machine Tools," *CIRP Annals - Manufacturing Technology*, **60**, pp 145–148.
- (11) Rawat, S. and Attia, H. (2009), "Wear Mechanisms and Tool Life Management of WC-Co Drills during Dry High Speed Drilling of Woven Carbon Fibre Composites," *Wear*, **267**, pp 1022–1030.
- (12) Gee, M. G., Gant, A., Hutchings, I., Bethke, R., Schiffman, K., Van Aker, K., Poulat, S., Gachon, Y., and von Sterbut, J. (2003), "Progress towards Standardisation of Ball Cratering," *Wear*, **255**, pp 1–13.
- (13) Ramalho, A. (2005), "Micro-Scale Abrasive Wear of Coated Surfaces—Prediction Models," *Surface and Coatings Technology*, **197**, pp 358–366.
- (14) Lou, D. B., Fridrici, V., and Kasper, Ph. (2010), "Relationships between the Fretting Wear Behavior and the Ball Cratering Resistance of Solid Lubricant Coatings," *Surface and Coatings Technology*, **204**, pp 1259–1269.
- (15) Duan, D. L., Li, S., Duan, X. H., and Li, S. Z. (2005), "Wear Behavior of Thermally Sprayed Coatings under Different Loading Conditions," *Tribology Transactions*, **48**, pp 45–50.
- (16) Sander, T., Tremmel, S., and Wartzack, S. (2011), "A Modified Scratch Test for the Mechanical Characterization of Scratch Resistance and Adhesion of Thin Hard Coatings on Soft Substrates," *Surface and Coatings Technology*, **206**, pp 1873–1878.
- (17) Li, J. and Beres, W. (2006), "Three-Dimensional Finite Element Modelling of the Scratch Test for a TiN Coated Titanium Alloy Substrate," *Wear*, **260**, pp 1232–1242.
- (18) Rawers, J. C., Tylczak, J. H., and Alman, D. E. (2008), "Wear Evaluation of High Interstitial Stainless Steels," *Tribology Transactions*, **51**, pp 515–525.
- (19) Bautista, Y., Gonzalez, J., Gilabert, J., Ibañez, M. J., and Sanz, V. (2011), "Correlation between the Wear Resistance, and the Scratch Resistance, for Nanocomposite Coatings," *Progress in Organic Coatings*, **70**, pp 178–185.